Supporting Information

Capacitance-soaring phenomenon induced by CuO electrode reconstruction with metastable $Cu(OH)_2$ nanowires

Jie Bai [a,b], Zhenhuai Yang [c]*, Qiang Wang [a,b]*

[a] School of Aeronautics, Chongqing Jiaotong University, Chongqing 400074, P. R. China

[b] Chongqing Key Laboratory of Green Aviation Energy and Power, The Green Aerotechnics Research Institute of Chongqing Jiaotong University, Chongqing 401120, P. R. China

[c] Laboratory of Microwave and Vacuum Technology, Jihua Laboratory, Foshan 528200, P. R. China

* Corresponding authors: Qiang Wang and Zhenhuai Yang

Email: wangq@cqjtu.edu.cn (Q. Wang), yangzhh@jihualab.ac.cn (Z. Yang)

Tel. / Fax: +86-023-47273962

Address: No.66 Xuefu Avenue, Nan'an District, Chongqing 400074 P.R. China

1. Experimental

1.1. Synthesis

The Cu foam used in the experiment was purchased from Kunshan Jiayisheng Electronics Co. Ltd. Potassium hydroxide (KOH) pellets, anhydrous ethanol, and deionized water were purchased from Harbin Baida Chemical Co. Ltd. Electrochemical reactions, and the performance tests were conducted using an electrochemical workstation (PGSTAT 302N) produced by Masson (China) Co. Ltd. $Cu(OH)_2$ nanowire

precursors were prepared through in-situ anodic oxidation on a Cu foam surface. A two-electrode system was used, with a Cu foam as the working electrode and Pt sheet as the counter and reference electrodes. Before the start of the experiment, the Cu foam (100 PPI, area 1 cm^{-2}), which was used as the Cu source and collector, was soaked in absolute ethanol and deionized water for ultrasonic cleaning for 15 min to remove impurities and pollutants from the surface. Then, the cleaned Cu foam was placed in deionized water for subsequent experiments. The KOH particles and deionized water were used to prepare a 3 M KOH aqueous solution as the electrolyte. The current density was 30 mA cm^{-2}, and the duration of the electrochemical reaction was 20 min. The prepared $Cu(OH)_2$ nanowire electrode was immersed in absolute ethanol and deionized water five times before being dried in an oven at 60 °C for 120 min. The experiments on the transformation of the $Cu(OH)_2$ nanowire precursors to CuO nanosheets were performed using a three-electrode system for electrochemical reactions. A Cu foam aggregate with $Cu(OH)_2$ nanowires grown on the surface was used as the working electrode. A Pt plate, saturated calomel electrode, and 3 M KOH aqueous solution were used as the counter electrode, reference electrode, and electrolyte for the electrochemical reaction, respectively. After 1,500 cyclic voltammetry (CV) cycles, the $Cu(OH)_2$ nanowire precursor was completely transformed into interconnected CuO nanosheets; that is, a composite electrode composed of CuO nanosheets and Cu foam was obtained.

1.2. Characterization

The surface morphology and microstructure of the synthesized samples were characterized by field-emission scanning electron microscopy (FEI Helios Nanolab 600i, operated at 5–20 kV) and transmission electron microscopy (FEI Tecnai G2 F30, operated at 300 kV). The crystal structures and chemical compositions of the prepared samples were characterized using X-ray diffraction (X' Pert Pro MRD) and X-ray photoelectron spectroscopy (Escalab 250Xi).

1.3. Electrochemical measurement

An electrochemical workstation (PGSTAT 302N, Metrohm Autolab B.V., the Netherlands) with a three-electrode cell was used for CV and galvanostatic charge–discharge (GCD) analyses at room temperature. The fabricated samples, Pt foil, and calomel acted as the working, counter, and reference electrodes, respectively, and a 6 M KOH aqueous solution was used as the electrolyte. The CV test was conducted at a potential window of 0.6 V and scan rate from 10–500 mV s^{-1}. The GCD test was conducted at current densities in the range 10–100 mA cm^{-2}. The 1,500 CV cycles of the prepared $Cu(OH)_2$ nanowire electrode were conducted at scan rate of 50 mV s^{-1} in a three-electrode system.

The specific capacitance (C_a; F cm^{-2}) of the electrode according to the CV curves at different scan rate was calculated using Eq. (1):

$$C_a = \frac{\int IdV}{2vS\Delta V} \quad (1)$$

where I (A) is the response current, V (V) is the potential, and v (mV s^{-1}), S (cm^{-2}), and ΔV (V) represent the scan rate, surface area of the electrode, and potential

window, respectively. The areal capacitance (C_A; F cm^{-2}) was calculated from GCD curves using Eq. (2):

$$C_A = \frac{I\int Vdt}{S\Delta V^2} \quad (2)$$

where I (A) is the discharge current, V (V) is the potential, t (s) is the discharge time, S (cm^{-2}) is the electrode surface area, and ΔV (V) is the working potential.

2. CuO nanosheets prepared without copper hydroxide nanowire precursors

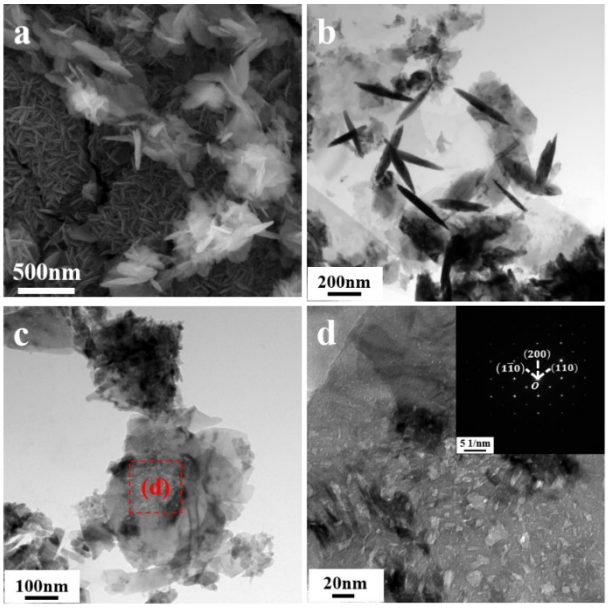

Fig. S1 (a) SEM image of CuO nanosheets prepared without copper hydroxide nanowire precursors. (b) TEM image of CuO nanosheets prepared without copper hydroxide nanowire precursors. (c) TEM image of fragment of prepared CuO nanosheet. (d) High-magnification TEM image of a CuO nanosheet fragment (inset is SAED image of the CuO nanosheet fragment in (c)).

The SEM image of CuO crystals obtained after 1500 CV cycles with copper foam base and copper source in a three-electrode system were shown in Fig. S1a. An elliptical vertical basis-oriented nanosheet structure is formed on the surface of the copper foam.

The nanosheets interlace with each other at different angles to form a three-dimensional network structure, which provides a large specific surface area for the diffusion of electrolyte ions and the transport of reactive substances. At sites with higher reactivity and local locations with higher ion concentration, the nanosheets were stacked with each other to form porous microspherical clusters. The nanosheets were wrapped around each other, and the diameter of the clusters was approximately 500 nm. Fig. S1b–d shows the TEM diagram of CuO nanosheet electrode prepared without $Cu(OH)_2$ nanowire precursors. Fig. S1b indicates that the surface of the electrode prepared without $Cu(OH)_2$ nanowire precursors is composed of two structures, one is an elliptical nanosheet stacked on top of each other, and the other is a spindle shaped structure. The selected area in the red box in Fig. S1c is a part of the elliptic nanosheet fragment, and the structure as shown in Fig. S1d is obtained after several cycles of magnification. A large number of holes with a diameter of approximately 2–10 nm is distributed on the surface of the nanosheet, and the existence of these holes is conducive to the passage of electrolyte ions. The illustration shows the diffraction spots of the nanoparticle. The diffraction spots of the regular arrangement indicate that the nanoparticle is a single crystal. However, because the nanoparticle is carved by holes of different sizes, the image of the boundary is not clear. Therefore, without $Cu(OH)_2$ nanowire precursors, CuO nanosheets can also be generated through CV cycle treatment, whose structure is perpendicular to the base and cross-linked with each other. Further, there is a large number of nanoholes on the surface of the generated CuO nanosheets. This multi-level

micro-/nanostructure increases the contact area with the electrolyte and is expected to yield better electrochemical energy storage capacity.

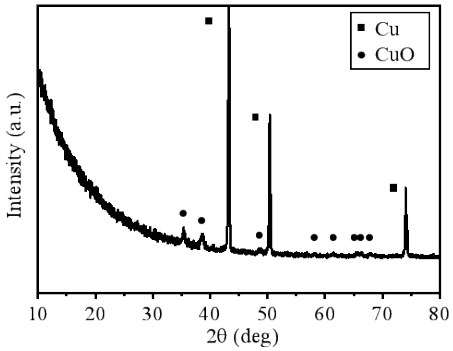

Fig. S2 XRD pattern of CuO nanosheets prepared without copper hydroxide nanowire precursors.

To clarify the crystal structure and phase composition of the electrode surface, XRD tests were conducted on the prepared electrode; the results are shown in Fig. S2. In addition to the diffraction peak of Cu indicated using a square symbol, the diffraction peak of CuO, indicated using a circular symbol, was also found. Moreover, no other crystal phase containing copper oxides or hydroxides was found, indicating the high purity of the prepared electrode. The 2θ values of 35.3°, 38.5°, 48.7°, 58.3°, 61.4°, 65.6°, 66.3° and 67.9° correspond to the diffraction peaks observed in the CuO crystals, namely, (002), (111), (202), (202), (113), (022), (311), and (113) crystal planes (PDF card #45-0937), respectively; this indicates the presence of CuO phase in the prepared electrode and good crystallinity.

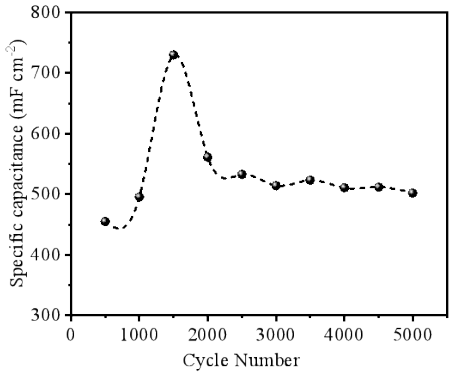

Fig. S3 Area-specific capacitance of CuO electrode prepared without copper hydroxide nanowire precursors after different CV cycle number at current density of 60 mA cm^{-2}.

As shown in Fig. S3, the area-specific capacitance of the CuO nanosheet electrode prepared without precursors first increases and then decreases as the number of CV cycles increases. After approximately 1,500 CV cycles, the area specific capacitance reaches a maximum of about 730 mF cm^{-2}, which is higher than the area specific capacitance (608 mF cm^{-2}) of CuO nanosheet electrodes prepared with $Cu(OH)_2$ nanowire precursors after 1500 CV cycles. This result may be attributed to the relatively high quality of CuO nanosheet crystals grown without precursors, which is consistent with the results of XRD tests. However, the capacitance-soaring phenomenon is not observed in the CuO nanosheet electrode prepared without $Cu(OH)_2$ nanowire precursors.

3. CuO nanosheet electrode after 10,000 charge–discharge cycles

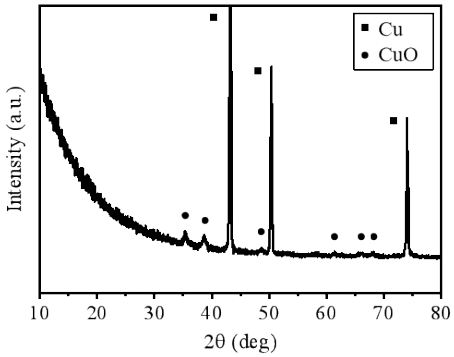

Fig. S4 XRD pattern of CuO nanosheet electrode after 10,000 charge–discharge cycles.

Fig. S4 shows the XRD pattern of the CuO nanosheet electrode prepared with $Cu(OH)_2$ nanowire precursors after 10,000 charge–discharge cycles at a current density of 60 mA cm^{-2}. As shown in Fig. S4, after 10,000 charge–discharge cycles, the electrode mainly contained Cu and CuO, and no crystal phase of other types of cupric oxide or hydroxide was found. The 2θ values of 35.3°, 38.5°, 48.7°, 61.4°, 66.3°, and 67.9° correspond to the diffraction peaks observed in CuO crystals, namely, (002), (111), (202), (113), (311), and (113) crystal planes, respectively (PDF card #45-0937), indicating the high purity of the CuO nanosheet electrode after 10,000 charge–discharge cycles.

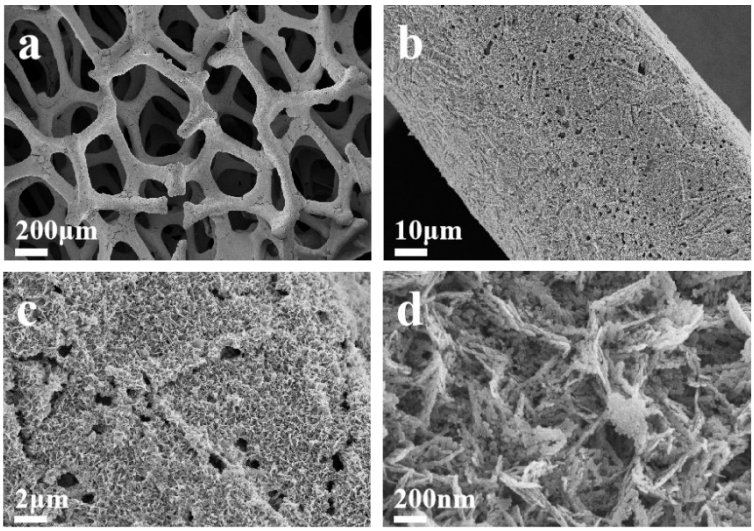

Fig. S5 SEM images of CuO nanosheet electrode prepared with $Cu(OH)_2$ nanowire precursors after 10,000 CV cycles at current density of 60 mA cm^{-2}. (a) Low-magnification SEM image. (b) SEM image of electrode skeleton. (c) SEM image of nanosheets. (d) High-magnification SEM image of nanosheets.

Surface morphology of the CuO nanosheet electrode after 10,000 charge–discharge cycles was characterized via SEM (Fig. S5). Fig. S5a shows that the electrode foam skeleton remains intact after 10,000 CV cycles. As shown in Figs. S5b and S5c, numerous pores are formed by CuO active substances on the electrode surface, and the nanosheet structures are also corroded into a large number of fragments (Fig. S5d); this is conducive to the infiltration of the electrolyte. However, the internal ion transport network channel is damaged. This is probably why after 10,000 charge–discharge cycles and with the electrode area ratio capacitance continuously increasing to nearly 3.2 times of the initial value, the capacitance finally begins to decay.